ACHIEVABLE ROBUSTNESS COMPARISON OF POSITION SENSED AND SELF-SENSING MAGNETIC BEARING SYSTEMS*

Nancy Morse Thibeault[†] Roy Smith[‡] Brad Paden[§] James Antaki[¶]

ABSTRACT

Two options for the control of a magnetic bearing system are considered and compared for achievable robustness. The first of these, the position sensed configuration, uses a measurement of the position of the rotor for feedback. The second configuration, the self-sensing configuration, attempts to achieve closed-loop stability and robustness using only a measurement of the electromagnet coil currents. We derive limits, independent of the choice of linear, time-invariant controller, on the achievable robustness in each case. We also consider how these limits change with changing bearing physical parameters as well as closed-loop system bandwidth and controller relative degree. Finally, we consider an example magnetic bearing system in order to determine the magnitude of these bounds for a real system.

*The authors would like to sincerely thank the McGowan Center for Artificial Organ Development and Magnetic Moments, LLC. for their financial support of this research. This work was also supported in part by NSF Grant ECS-9634498.

[†]Department of Mechanical Engineering, University of California at Santa Barbara, Santa Barbara, CA 93106-5070, nancy@engineering.ucsb.edu

[‡]Department of Electrical and Computer Engineering, University of California at Santa Barbara, Santa Barbara, CA 93106-2040, roy@ece.ucsb.edu

[§]Magnetic Moments LLC., 5733C Hollister Ave., Goleta, CA 93117, bpaden@mmsb.com

[¶]University of Pittsburg, 420 Center for Biotechnology and Bioengineering, 300 Technology Dr., Pittsburg, PA 15219, antaki@pittsurg.nb.upmc.edu

1 INTRODUCTION

Commonly used sensors, for the purpose of controlling a magnetic bearing system, are position sensors and current sensors. Position measurement is attractive because it provides direct information on the system property which is typically most important to regulate, the rotor position. However, achieving closed-loop stability by current measurement alone (known as the self-sensing bearing configuration) is desirable because of the low cost and simplicity of current sensors. Attracted by these potential benefits, many researchers have studied and implemented magnetic bearings using the self-sensing configuration [1]-[5]. However, these investigations have typically **shown** this configuration to yield low robustness to system unmodeled dynamics [1]-[6]. In the following development, we will offer an explanation of these findings by showing that the self-sensing configuration is particularly limited in its achievable robustness for any internally stabilizing, linear, time-invariant (LTI) controller. We show that these robustness limitations increase further with constraints placed on the closed-loop system bandwidth and controller relative degree. We will also investigate how the choice of magnetic bearing system parameters affects these robustness limits. In addition, we derive bounds on achievable robustness for the position sensed magnetic bearing configuration; however, we show that these bounds are typically much less restrictive than in the self-sensing case.

2 BASIC MAGNETIC BEARING SYSTEM MODEL

The system we will consider is the two-pole, single degree-of-freedom magnetic bearing shown in Figure 1. This system represents the fundamental building block for many more complicated magnetic bearing systems, and, as such, it offers the essential design challenges associated with magnetic bearings without unnecessary complexity. For our model derivation, we will make the following assumptions about our system. We assume that the levitated bar moves in only one degree-of-freedom, the x direction. In addition, we do not allow for any rotation or bending of the bar. This leads us to conclude that the gap lengths G_1 and G_2 must be the same when measured from either pole of the given electromagnet. The point at which $G_1 = G_2$, centered between the electromagnets, is an unstable equilibrium point; thus, active feedback control is required to achieve stability about this point. A list of the bearing system parameters is included in Table 1.

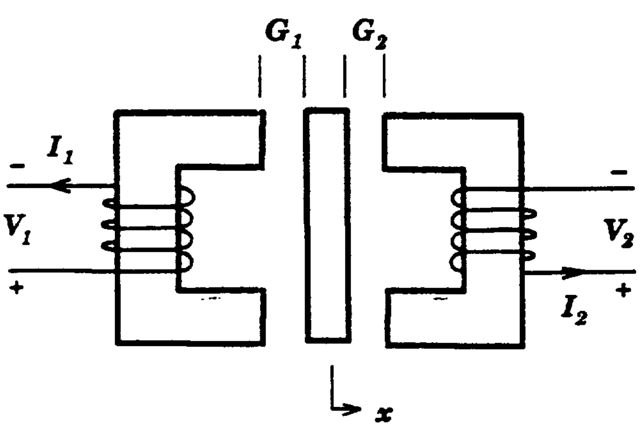

Figure 1: Two Electromagnet Magnetic Bearing System

A linearization of the bearing dynamics about the operating point

Symbol	*Description*
μ_0	Permeability of air
N	The number of turns in each coil
A_g	Cross sectional area of the air gap
m	Mass of the bar
G_0	The nominal gap value
R	The resistance of each coil
I_0	The bias current
V_0	The bias voltage
L	The coil inductance $L = \frac{\mu_0 N^2 A_g}{2G_0}$
k_I	The current force constant $k_I = \frac{2LI_0}{mG_0}$
k_x	The position force constant $k_x = k_I \frac{I_0}{G_0}$

Table 1: Magnetic Bearing Parameters

$$\begin{bmatrix} x & \dot{x} & I_1 & I_2 & \dot{I}_1 & \dot{I}_2 \end{bmatrix}^T = \begin{bmatrix} 0 & 0 & I_0 & -I_0 & 0 & 0 \end{bmatrix}^T, \quad (1)$$

where I_0 is a constant bias current, and making the following definitions $I_c := (I_1 + I_2)/2$ and $V_c := (V_1 + V_2)/2$, yields the linearized bearing system model:

$$\ddot{x} = k_x x + k_I I_c \quad (2)$$

$$\dot{I}_c = -\frac{R}{L} I_c - \frac{I_0}{G_0}\dot{x} + \frac{1}{L} V_c. \quad (3)$$

For this system there are several choices of measured outputs. In this paper we will analyze and compare two measurement configurations. The first uses a measurement of the rotor position x. We will refer to this as the Position Measurement (PM) configuration. Another output option is to measure the current I_c. We refer to this as the Current Measurement (CM) (or Self-Sensing) configuration. Transfer function representations of the PM and CM configurations, respectively, are given below.

$$y_{PM}(s) = x(s) = \frac{\frac{k_L}{L}}{s^3 + \frac{R}{L}s^2 - \frac{R}{L}k_x} V_c(s) \quad (4)$$

$$y_{CM}(s) = I_c(s) = \frac{\frac{1}{L}(s^2 - k_x)}{s^3 + \frac{R}{L}s^2 - \frac{R}{L}k_x} V_c(s) \quad (5)$$

Both of these transfer functions are controllable and observable and share the characteristic equation $s^3 + \frac{R}{L}s^2 - \frac{R}{L}k_x$ which has one real, unstable pole which we will denote p_0, and two other stable poles. The CM configuration, a SISO system, has a real, non-minimum phase (NMP) zero located at $s = \sqrt{k_x}$ which we denote z_0. The PM system has no finite transmission zeros.

We next consider the closed-loop system with P, representing the magnetic bearing system in either the PM or CM configuration, in feedback with the controller, C. This closed-loop system has a loop gain of $L = PC$ along with sensitivity and complementary sensitivity functions S and T as follows:

$$S(s) := \frac{1}{1 + L(s)} \qquad T(s) := \frac{L(s)}{1 + L(s)}. \quad (6)$$

From this we see that the poles of L are zeros of S and the zeros of L are zeros of T. Therefore, the following relationships hold: $S(p_0) = 0$, $T(p_0) = 1$. In the CM configuration, the following relationships also hold: $S^{CM}(z_0) = 1$, and $T^{CM}(z_0) = 0$.

In the following development, we will investigate certain limits on the achievable sensitivity and complementary sensitivity reduction which result from the interpolation conditions on S and T given above. Additional constraints on S and T can be derived by considering their behavior at high frequencies. For practical systems, $L(j\omega) \to 0$ as $\omega \to \infty$. Thus, $S = \frac{1}{1+L(s)} \to 1$ and $T = \frac{L(s)}{1+L(s)} \to 0$ as $\omega \to \infty$. In fact, not only are the magnitudes of S and T bounded at high frequencies but also the rate of convergence of each is bounded, the rate bound depending on the relative degree of L. These high frequency constraints on S and T can provide additional robustness and performance limits for our magnetic bearing system as we will show in the development that follows. The following constraint, adapted from [10], will be imposed upon our magnetic bearing system to determine the effect of such high frequency affects as finite closed-loop system bandwidth and non-zero controller relative degree on the achievable robustness of our system.

Constraint 1 *Let ω_c be equal to the desired bandwidth of T and let k be a non-negative integer equal to the relative degree of L. Then given $\rho \in \mathbb{R}$, $1 \geq \rho > 0$, let S and T be constrained in high frequencies as follows:*

$$|S(j\omega) - 1| = |T(j\omega)| \leq \rho \left(\frac{\omega_c}{\omega}\right)^k \qquad \forall \omega \geq \omega_c. \quad (7)$$

In the analysis that follows, we will employ the $\mathcal{H}_\infty$ system norm which is defined for a stable, LTI, SISO system $G(s)$ as follows:

$$\|G\|_\infty := \sup_{\omega \in \mathbf{R}} |G(j\omega)|.$$

3 MEASURES OF ROBUSTNESS

We now introduce two measures of robustness based on the sensitivity and complementary sensitivity functions. We will use these robustness measures in the following development to bound the achievable robustness of our various system configurations.

A classical measure of robustness for SISO systems is the distance from the Nyquist plot of the system loop transfer function L to the critical point $(-1, 0)$. This distance is exactly $\frac{1}{\|S\|_\infty}$. Therefore, large values of $\|S\|_\infty$ imply poor robustness for SISO systems.

Similarly, constraints of the form $\|T(s)\|_\infty \geq \beta$ are directly linked to classical gain and phase margin ideas of robustness for both MIMO and SISO systems. The block diagram of Figure 2 represents our magnetic bearing system model P, perturbed as $P(1+\Delta)$ where Δ is an unknown, norm bounded perturbation. The transfer function seen by Δ, an output multiplicative uncertainty in the plant, is simply $-T$. Thus, from the small gain theorem [13],

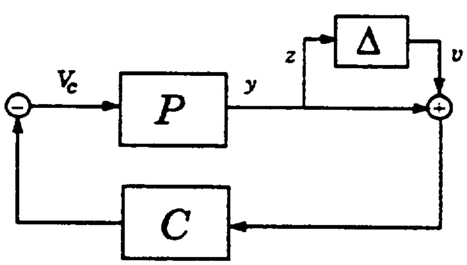

Figure 2: Bearing System with Output Multiplicative Perturbation

we have the following result.

Remark 2: Output Multiplicative Stability Margin *The system of Figure 2 is guaranteed to remain stable for all unknown bounded systems Δ such that*

$$\|\Delta\|_\infty < \frac{1}{\|T\|_\infty} \qquad (8)$$

and there exists a destabilizing LTI system Δ satisfying:

$$\|\Delta\|_\infty = \frac{1}{\|T\|_\infty}. \qquad (9)$$

4 ROBUSTNESS LIMITS OF THE PM CONFIGURATION

4.1 SENSITIVITY BOUNDS

The PM system is a SISO system with an unstable pole. Therefore, the following integral constraint on the sensitivity function holds [9]:

$$\int_0^\infty \log|S^{PM}(j\omega)|d\omega = \pi p_0. \qquad (10)$$

Since $p_0 \in \mathbb{R}$, $p_0 > 0$, this constraint tells us that for some frequency range, $|S^{PM}(j\omega)| > 1$. Thus,

$$\|S^{PM}\|_\infty > 1. \qquad (11)$$

If we constrain S^{PM} at high frequencies as given in Constraint 1, the peak magnitude of S^{PM} overall increases. The following theorem characterizes this phenomenon more precisely.

Theorem 3 *Consider P to be the linear model of our PM magnetic bearing system given in (4) with unstable pole p_0. Assume C is an LTI, internally stabilizing controller for our system in feedback as shown in Figure 2. Denote the sensitivity function for this closed-loop system as S^{PM} defined as in (6) and assume that the high frequency bounds of Constraint 1 apply. Then the following bound holds:*

$$\|S^{PM}\|_\infty \geq e^{\left[\frac{\pi p_0}{\omega_c} - \frac{1}{\omega_c}\int_{\omega_c}^\infty \log\left[\rho\left(\frac{\omega_c}{\omega}\right)^k + 1\right] d\omega\right]}.$$

Proof: The proof combines the procedure outlined in the proof of Theorem 3 of [9] with the high frequency constraint analysis of [10]. ■

Note that the bound derived above on $\|S^{PM}\|_\infty$ requires the condition that $k \geq 2$. However, since k is the relative degree of L and P^{PM} itself has a relative degree of 3, this condition is always satisfied.

4.2 COMPLEMENTARY SENSITIVITY BOUNDS

Since our PM magnetic bearing system is an unstable, minimum-phase system, we may use Lemma A.1 of [9], to deduce the following bound:

$$||T^{\text{PM}}||_\infty > 1 \tag{12}$$

Note: To derive this bound, we make the assignment $f(s) = T^{\text{PM}}(s)$ in Lemma A.1 of [9] and employ the fact that $T^{\text{PM}}(p_0) = 1$.

With the application of high frequency constraints on T, its lower bound will increase further as shown in the following theorem.

Theorem 4 *Consider P to be the linear model of our PM magnetic bearing system given in (4) and p_0 its unstable pole. Assume C is an LTI, internally stabilizing controller for our system connected as shown in Figure 2. Denote the closed-loop complementary sensitivity function as T^{PM} defined as in (6) and assume that the high frequency bounds of Constraint 1 apply. Then if we define*

$$\begin{aligned}
\phi_c &:= \tan^{-1}(\omega_c/p_0)\\
\alpha &:= \frac{\pi/2}{\phi_c}\\
Cl_2(\theta) &:= -\int_0^\theta \log\left(2\sin\frac{z}{2}\right)dz\\
I(\phi_c) &:= Cl_2(2\phi_c) + Cl_2(\pi - 2\phi_c)
\end{aligned}$$

where Cl_2 is the Clausen integral [11], the following bound results:

$$||T^{\text{PM}}||_\infty \geq \left(\frac{1}{\rho}\right)^{(\alpha-1)} \left[\left(\frac{p_0}{\omega_c}\right)^{(\alpha-1)} e^{\frac{I(\phi_c)}{2\phi_c}}\right]^k.$$

Proof: The proof of this result combines the analysis of Theorem 2 of [10] with that of Equation (12) above. ∎

5 ROBUSTNESS LIMITS OF THE CM CONFIGURATION

5.1 SENSITIVITY BOUNDS

Through the application of Poisson's integral formula, Freudenberg and Looze [9] derive the following bound on the sensitivity function of any linear, time-invariant system, such as our linearized bearing system in the CM configuration, with an unstable pole p_0 and a NMP zero z_0 that is stabilized by a linear, time-invariant controller.

$$||S^{\text{CM}}||_\infty \geq \left|\frac{p_0 + z_0}{p_0 - z_0}\right| \tag{13}$$

Notice that this bound becomes infinite as p_0 and z_0 approach each other.

If we constrain S^{CM} at high frequencies as given in Constraint 1, then we obtain the following bound on the sensitivity function which, as we will show later using a practical example, can be a more restrictive bound than Equation (13).

Theorem 5 *Consider P to be the linear model of our CM magnetic bearing system given in (5) and C to be an LTI, internally stabilizing controller for our system in feedback as shown in Figure 2. Denote the sensitivity function for this closed-loop system as S^{CM} defined as in (6) and assume that the high frequency bounds of Constraint 1 apply. Let p_0 and z_0 denote the RHP pole and zero of P, respectively. Then if we define*

$$\begin{aligned}
\beta &:= \frac{\pi/2}{\psi_c}\\
\psi_c &:= \tan^{-1}(\omega_c/z_0)\\
d\theta_{z_0}(\omega) &:= \frac{z_0}{z_0^2 + \omega^2}d\omega,
\end{aligned}$$

the following bound holds:

$$||S^{\text{CM}}||_\infty \geq \left|\frac{p_0 + z_0}{p_0 - z_0}\right|^\beta e^{\left[-\frac{1}{\psi_c}\int_{\omega_c}^{\infty} \log\left[\rho\left(\frac{\omega_c}{\omega}\right)^k + 1\right] d\theta_{z_0}(\omega)\right]}.$$

Proof: The proof is a simple modification of Theorem 1 of Freudenberg and Looze [9]. ■

5.2 COMPLEMENTARY SENSITIVITY BOUNDS

Bounds on complementary sensitivity can be derived using similar techniques. From Looze and Freudenberg [10], we have for our CM configuration:

$$\|T^{CM}\|_\infty \geq \left|\frac{z_0 + p_0}{z_0 - p_0}\right|. \qquad (14)$$

Additionally, Looze and Freudenberg [10] show that high frequency limitations on the magnitude and convergence rate of T^{CM} further constrain the achievable complementary sensitivity reduction. If we bound T^{CM} at high frequencies as shown in Constraint 1, we obtain the following bound on the achievable $\|T^{CM}\|_\infty$.

Theorem 6 *Consider P to be the linear model of our CM magnetic bearing system given in (5) and C to be an LTI, internally stabilizing controller for our system connected as shown in Figure 2. Denote the closed-loop complementary sensitivity function as T^{CM} defined as in (6) and assume that the high frequency bounds of Constraint 1 apply. Let p_0 and z_0 denote the RHP pole and zero of P, respectively. Then if we define*

$$\phi_c := \tan^{-1}(\omega_c/p_0)$$
$$\alpha := \frac{\pi/2}{\phi_c}$$
$$Cl_2(\theta) := -\int_0^\theta \log\left(2\sin\frac{z}{2}\right)dz$$
$$I(\phi_c) := Cl_2(2\phi_c) + Cl_2(\pi - 2\phi_c)$$

where Cl_2 is the Clausen integral [11], the following bound results:

$$\|T^{CM}\|_\infty \geq \left(\left|\frac{z_0 + p_0}{z_0 - p_0}\right|\right)^{\alpha} \left(\frac{1}{\rho}\right)^{(\alpha-1)} \times \left[\left(\frac{p_0}{\omega_c}\right)^{(\alpha-1)} e^{\frac{I(\phi_c)}{2\phi_c}}\right]^k.$$

Proof: This proof closely parallels that given in Theorem 2 of [10]. ■

Notice the similarity of these bounds with the PM bounds given in Section 4. For the CM bounds, the term $\left|\frac{z_0+p_0}{z_0-p_0}\right|$ replaces the quantity 1 in the PM bounds. Thus, the CM bounds are typically much larger than the PM bounds.

6 DESIGN IMPLICATIONS

In order to give realistic numerical values to the robustness and performance limitations derived above, we evaluate them for a real magnetic bearing system. For this purpose, we consider the MBC500 magnetic bearing system [8] which has the parameter values given in Table 2. For a magnetic bearing system with these parameter values, the unstable pole and non-minimum phase zero are, respectively,

$$p_0 = 248.55 \text{ rad/sec} \qquad z_0 = 295.73 \text{ rad/sec}.$$

μ_0	: $4\pi \times 10^{-7}\frac{\text{Wb}}{\text{A}\cdot\text{m}}$	R	: 2.2 ohms
N	: 220 turns	I_0	: 0.5 A
A_g	: 4.84×10^{-5} m^2	L	: 3.68 mH
m	: 0.1315 kg	k_I	: $7.00 \times 10^4 \frac{\text{mm}}{\text{A}\cdot\text{s}^2}$
G_0	: 0.4 mm	k_x	: $8.74 \times 10^4 \frac{1}{\text{s}^2}$

Table 2: MBC500 Magnetic Bearing Parameter Values

Table 3 below contains an evaluation of the bounds on $||S||_\infty$ and $||T||_\infty$ given in Equations (11), (12), (13) and (14) for both magnetic bearing configurations assuming no high frequency constraints on $S(j\omega)$ and $T(j\omega)$ and given the parameter values specified in Table 2. In addition, it gives a value of $||S||_\infty$ and $||T||_\infty$ which has been achieved by solving a μ-Synthesis design and optimizing either $||S||_\infty$ or $||T||_\infty$. Notice that the lower bound values and the achieved norms differ by only a small amount for each configuration. This indicates that the lower bounds capture accurately the fundamental system properties that are limiting the achievable sensitivity or complementary sensitivity reduction in each configuration.

	CM Bearing	*PM Bearing*
$\|\|S\|\|_\infty$ *Lower Bound*	11.538	1
$\|\|T\|\|_\infty$ *Lower Bound*	11.538	1
$\|\|S\|\|_\infty$ *Achieved*	11.578	1.0235
$\|\|T\|\|_\infty$ *Achieved*	11.564	1.0349

Table 3: Upper and Lower Bounds on $||S||_\infty$ and $||T||_\infty$ for each Configuration

6.1 ROBUSTNESS LIMIT EVALUATIONS

6.1.1 PM CONFIGURATION:

All magnetic bearings in the PM configuration stabilized by an LTI controller satisfy the following bounds:

$$||S^{PM}||_\infty \geq 1 \quad \text{and} \quad ||T^{PM}||_\infty \geq 1 \tag{15}$$

as we showed in Equations (11) and (12). Furthermore, the sensitivity and complementary sensitivity bounds of the PM configuration are affected by high frequency magnitude constraints of the type given in Constraint 1 as shown in Theorems 3 and 4. Figures 3 and 4 show how these lower bounds on $||S^{PM}||_\infty$ and $||T^{PM}||_\infty$ are affected by choice of ω_c, ρ and k. Notice that the most significant factor leading to high sensitivities is the closed-loop bandwidth ω_c. The highest bounds occur when low ω_c is combined with high k or low ρ values. This is simply the classic "water bed" effect.

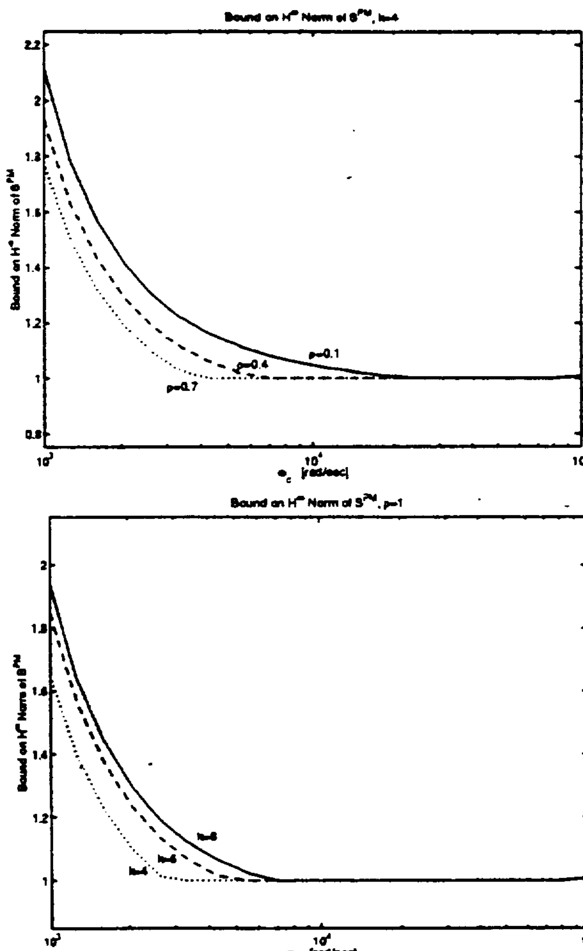

Figure 3: Bound on PM Configuration $||S^{PM}||_\infty$ for Varying ω_c, ρ and k

6.1.2 CM CONFIGURATION:

The plots given in Figure 5 show how the

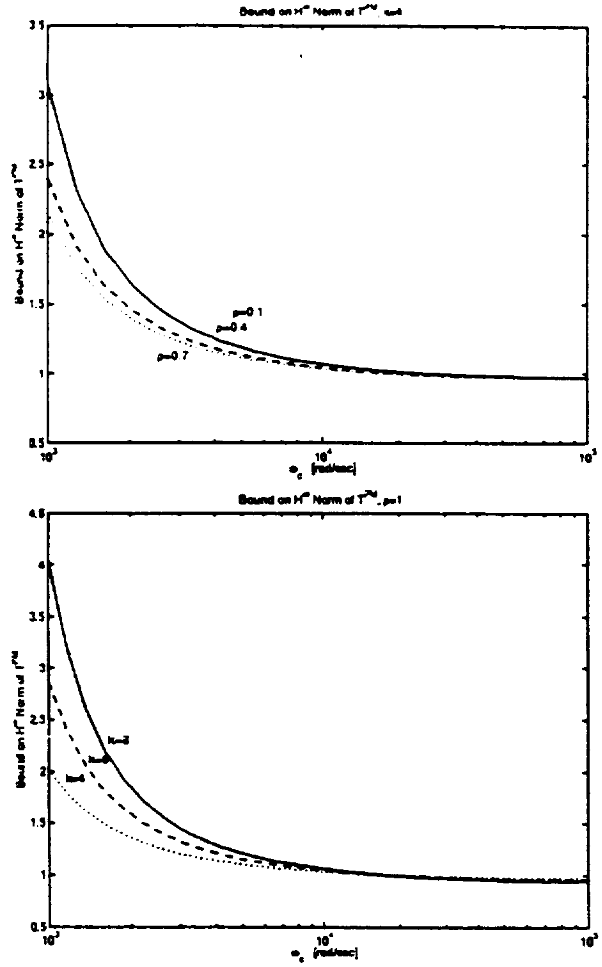

Figure 4: Bound on PM Configuration $||T^{\mathrm{PM}}||_\infty$ for Varying ω_c, ρ and k

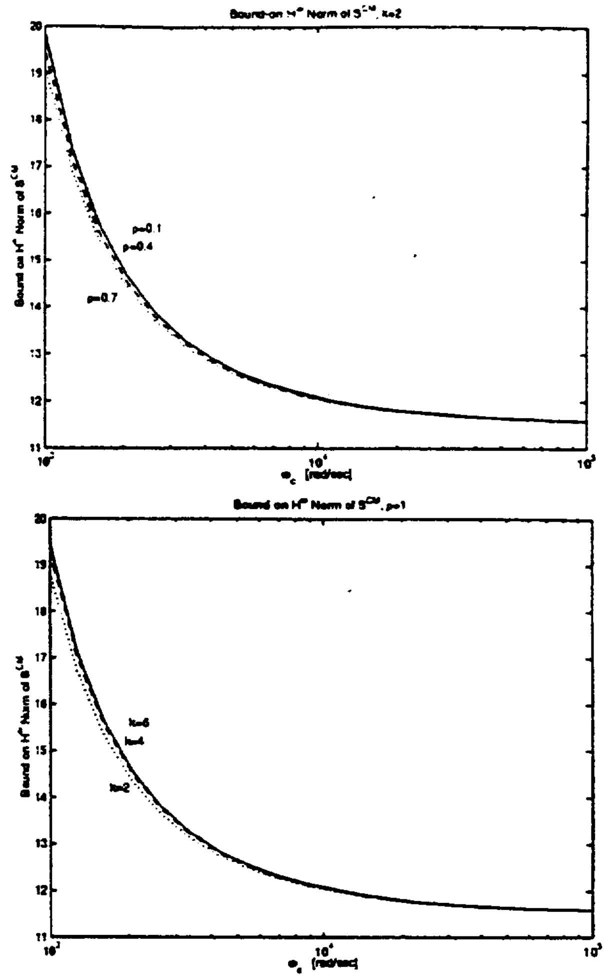

Figure 5: Bound on CM Configuration $||S^{\mathrm{CM}}||_\infty$ for Varying ω_c, ρ and k

bound on $||S^{\mathrm{CM}}||_\infty$ in Theorem 5 for the CM system varies with different values of ω_c, ρ and k. Similarly, Figure 6 shows how the bound on $||T^{\mathrm{CM}}||_\infty$ from Theorem 6 varies as we change ω_c, ρ and k. Again, the largest factor affecting peaks in S^{CM} and T^{CM} in Figures 5 and 6 is low closed-loop bandwidth ω_c. In addition, combining low ω_c with small values of ρ or high values of k produce especially high peaks. This has important implications for controller design. A primary reason for choosing the CM configuration is the low cost associated with having no position sensor. However, if high bandwidth is required in order to achieve acceptable robustness and performance, then the configuration may cease to be a low cost option.

We now consider the effect of varying the bearing system parameters on the sensitivity and complementary sensitivity bounds. We first make the observation that in the CM case, both $||S^{\mathrm{CM}}||_\infty$ and $||T^{\mathrm{CM}}||_\infty$ are bounded by the same quantity. Define

$$B_{CM} := \left|\frac{p_0 + z_0}{p_0 - z_0}\right|. \qquad (16)$$

From equations (13) and (14) we see that $||S^{\mathrm{CM}}||_\infty \geq B_{CM}$ and $||T^{\mathrm{CM}}||_\infty \geq B_{CM}$. Figure 7 shows how this lower bound on both

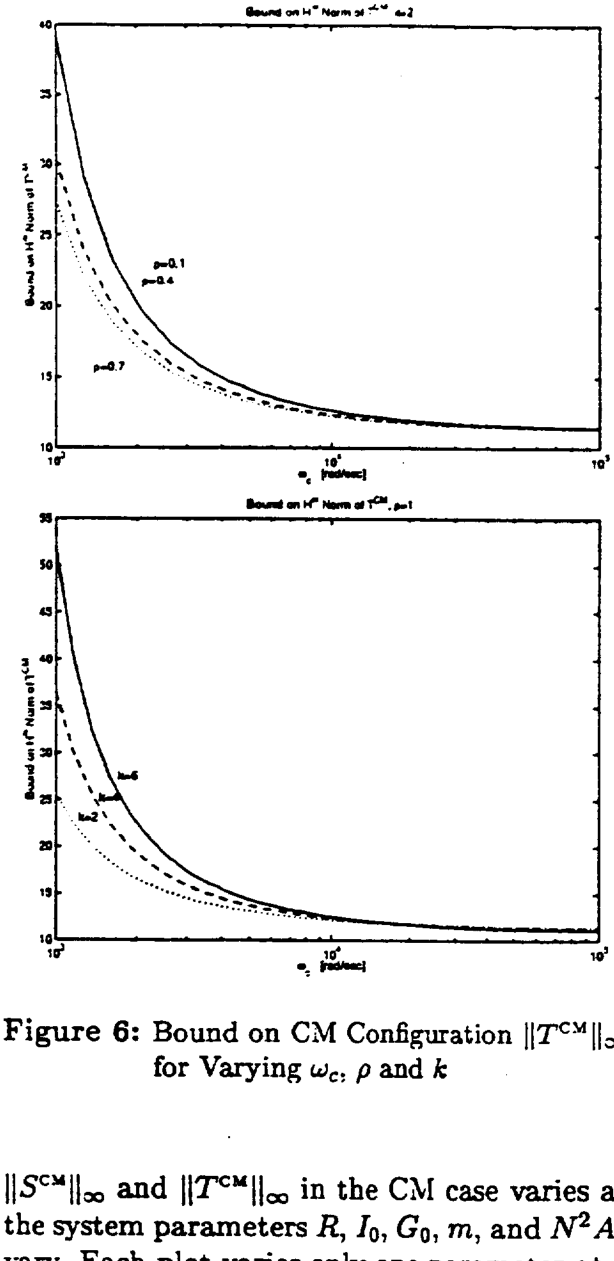

Figure 6: Bound on CM Configuration $\|T^{\text{CM}}\|_\infty$ for Varying ω_c, ρ and k

$\|S^{\text{CM}}\|_\infty$ and $\|T^{\text{CM}}\|_\infty$ in the CM case varies as the system parameters R, I_0, G_0, m, and N^2A_g vary. Each plot varies only one parameter at a time, spanning a range of ±50% of its nominal MBC500 bearing system value, while holding the other parameters fixed at the value used in the MBC500 bearing system.

All magnetic bearing systems have some inefficiency due to eddy currents, hysteresis, flux leakage, etc. For practical magnetic bearing systems, a constant γ called a derating factor, multiplying the force dynamics as shown below, is used to account for this loss in the system.

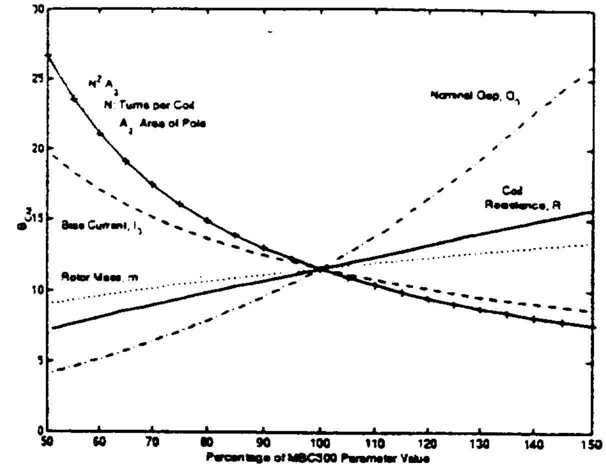

Figure 7: Bound on CM Configuration $\|S^{\text{CM}}\|_\infty$ and $\|T^{\text{CM}}\|_\infty$ for Varying Bearing Parameters R, I_0, G_0, m, and N^2A_g

$$\ddot{x} = \gamma(k_x x + k_I I_c) \tag{17}$$

Figure 8 shows how the bound on $\|S^{\text{CM}}\|_\infty$ and $\|T^{\text{CM}}\|_\infty$ varies as γ varies from 0.5 to 1. Typical values for this derating factor are 0.6 or 0.7. Note from Figure 8 that for the MBC500 bearing system in the CM configuration, a derating factor of 0.6 causes a 21% increase in B_{CM} from its underated value.

All of the plots in Figures 7 and 8 consider only one parameter varying at a time; however, to get an accurate view of the best and worst that the sensitivity and complementary sensitivity bounds can be in the CM case, we must vary all of the parameters simultaneously. Varying R, I_0, G_0, m, N^2A_g and γ simultaneously within the ranges plotted in Figures 7 and 8 we find the following best and worst case bounds, respectively:

$$B_{CM} = 2.0445 \quad \text{and} \quad B_{CM} = 337.22. \tag{18}$$

Now considering B_{CM} as a bound on $\|S^{\text{CM}}\|_\infty$, in the case of $B_{CM} = 2.0445$, the Nyquist plot

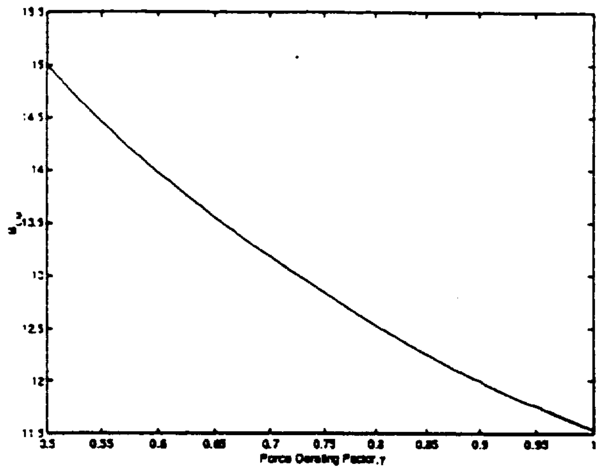

Figure 8: Bound on CM Configuration $\|S^{CM}\|_\infty$ and $\|T^{CM}\|_\infty$ for Varying Derating Factor, γ

for this system passes with a ball of radius $\frac{1}{2.0445} \approx 0.5$ of the critical point. The Nyquist plot associated with the CM system of bound $B_{CM} = 337.22$, however, passes within a ball of radius $\frac{1}{337.22} \approx 0.003$ of the critical point representing very poor robustness. Thus, the choice of the bearing dimensions and other physical properties can be critical to the achievable robustness of the controlled system when using the CM configuration.

7 CONCLUSION

The CM magnetic bearing configuration, although lower in cost and simpler to build than a PM bearing system, suffers from lower robustness to modeling uncertainties. The above analysis shows theoretically the reasons for reduced robustness in the CM case, that is, a near unstable pole/zero cancelation which causes the rotor position to be nearly unobservable in this configuration. In fact, limits have been given, which can be computed for any bearing system under consideration, which bound the robustness achievable by any linear controller in feedback with the linearized bearing model in the CM configuration. We have shown, by considering the MBC500 bearing system as a typical example, that the difference in these limits between the CM and PM configurations can be significant.

However, we also saw in (18) and Figures 7 and 8 that the robustness limitations for the CM configuration can vary significantly with changing bearing physical parameters and system properties such as closed-loop system bandwidth and controller relative degree. Using the analysis provided above, a magnetic bearing designer can use constraints on the physical properties of a given bearing system along with available controller bandwidth information, and closed-loop robustness requirements to determine if the CM configuration is a viable control option for a given application.

ACKNOWLEDGMENT

The authors would like to thank Jim Freudenberg, University of Michigan at Ann Arbor, for helpful discussions related to this research.

References

[1] Vischer, D. and H. Bleuler, "A New Approach to Sensorless and Voltage Controlled AMBs Based on Network Theory Concepts," Proceedings of the Second International Symposium on Magnetic Bearings, July 12-14, 1990, pp. 301-306.

[2] Bleuler, H., D. Vischer, G. Schweitzer, A. Traxler and D. Zlatnik, "New Concepts for Cost-Effective Magnetic Bearing Control," Automatica, Vol. 30, No. 5, 1994, pp. 871-876.

[3] Mizuno, T., H. Bleuler, H. Tanaka, H. Hashimoto, F. Harashima, H. Ueyama, "Industrial Application of Position Sensorless Active

Magnetic Bearings," Electrical Engineering in Japan, Vol. 117. No. 5, 1996, pp. 124-133.

[4] Mohamed. A. M, F. Matsumura. T. Namerikawa, J. Lee, "Modeling and Robust Control of Self-Sensing Magnetic Bearings with Unbalance Compensation," Proceedings of the 1997 IEEE International Conference on Control Applications, October 1997, pp. 586-594.

[5] Noh, M. D., E. H. Maslen, "Self-Sensing Magnetic Bearings Using Parameter Estimation," IEEE Transactions on Instrumentation and Measurement, Vol. 46, No. 1, February 1997, pp. 45-50.

[6] Kucera, L. "Robustness of Self-Sensing Magnetic Bearing," Magnetic Bearings Industrial Conference, Alexandria, USA, 1997. Also available on the web: http://www.ifr.mavt.ethz.ch/ifr.html.

[7] Havre, K. and S. Skogestad, "Effect of RHP Zeros and Poles on Performance in Multivariable Systems," Proceedings of the UKACC International Conference on Control '96, Exeter, UK, Sept. 1996, pp. 491-496.

[8] Paden, B., N. Morse, and R. Smith, "Magnetic Bearing Experiment for Integrated Teaching and Research Laboratories," Proceedings of the 1996 IEEE International Conference on Control Applications, Dearborn, MI, Sept. 15-18, 1996, pp. 421-425.

[9] Freudenberg, J. S. and D. P. Looze, "Right Half Plane Poles and Zeros and Design Tradeoffs in Feedback Systems," IEEE Transactions on Automatic Control, Vol. AC-30, No. 6, June 1985.

[10] Looze, D. P. and J. S. Freudenberg, "Limitations of Feedback Properties Imposed by Open-Loop Right Half Plane Poles," IEEE Transactions on Automatic Control, Vol. 36, No. 6, June 1991.

[11] Prudnikov, A. B., Yu A. Brychkov, and O. I. Marichev, *Integral and Series, Volume I: Elementary Functions*, New York, Gordon and Breach, 1986, Translated from *Inegraly i ryady*, Moscow, Nauka.

[12] Gómez, G. I. and G. C. Goodwin, "Integral Constraints on Sensitivity Vectors for Multivariable Systems," Automatica, Vol. 32, No. 4, pp.499- 518, 1996.

[13] Zhou, Kemin, J. Doyle, and K. Glover, *Robust and Optimal Control*, Printice Hall, 1996, pp. 217-219.